

Electron focusing in two-dimensional electron gases grown on (311)*B* GaAs substrates

A. C. Churchill, G. H. Kim, M. Y. Simmons, D. A. Ritchie, and G. A. C. Jones
Cavendish Laboratory, University of Cambridge, Madingley Road, Cambridge CB3 0HE, United Kingdom
 (Received 12 July 1994)

We present a study of electron focusing in two-dimensional electron gases grown on (311)-orientated GaAs substrates. The electronic properties of electron and hole gases grown on (311)-orientated GaAs substrates have anisotropic behavior in the orthogonal $[\bar{2}33]$ and $[01\bar{1}]$ directions, however, the electron focusing results presented demonstrate anisotropic effective mass and Fermi surface even though the mobility is anisotropic. We also determine the ballistic length for the electrons.

In this paper we present transverse electron-focusing studies of two-dimensional electron gases (2DEG's) grown on (311)*B* GaAs substrates. Transverse electron focusing has been used quite extensively to determine the shape of the Fermi surface, while originally used for metals,^{1,2} the idea has been transferred to the study of 2DEG's in GaAs/Al_xGa_{1-x}As structures³⁻⁵ and more recently two-dimensional hole gases (2DHG's).⁶ In the latter case the 2DHG's were grown on (311)*A*-orientated GaAs substrates.^{7,8} We have studied electron gases grown on (311)*B* GaAs substrates and found that, similarly to the 2DHG's grown on (311)*A*, there is a marked anisotropy in the transport properties: specifically the mobility in the $[\bar{2}33]$ direction can be 50% higher than in the $[01\bar{1}]$ direction.^{9,10} Heremans, Santos, and Shayegan, from their results for transverse hole focusing, suggest that the anisotropic mobilities can be explained by a warped Fermi surface that gives rise to a directional dependence of hole wave-vector magnitude and corresponding effective mass. Hole transport in 2D GaAs/Al_xGa_{1-x}As heterojunctions is in coupled light- and heavy-hole bands, which can give rise to anisotropic effective hole masses in various directions; however, this is not enough to explain the warping of the Fermi surface that they observe, which can be as high as 30%. They suggest that the effect is possibly caused by a modulation in the growth plane of the band structure, which is possibly caused by a surface corrugation on the (311) growth surface. There now seems to be some evidence that the surface of a (311) substrate is corrugated at temperatures typical of molecular-beam epitaxy (MBE) growth. This includes reflection high-energy electron-diffraction (RHEED) studies of the growth surface¹¹ and independent measurements on transport properties of electrons and holes in heterojunction systems;^{9,10} however, reports where both RHEED and electron properties have been studied systematically on the same sample are not yet available. In our investigations of the anisotropic mobility of 2DEG's on (311)*B* substrates,¹⁰ we found that the mobility dependence on carrier concentration could be explained by a model of anisotropic interface roughness scattering. However, anomalous magnetoresistance, which was also observed in these structures, suggested some merit in the idea of a band-structure modulation by

surface corrugations. As a further study we have fabricated an electron-focusing device similar to that of the hole focusing device of Heremans, Santos, and Shayegan, which not only allows us to determine the shape of the Fermi surface but also a ballistic length for electrons in the 2DEG.

Figure 1 shows a schematic of the device; the undoped (311)*B* wafers were grown in a Varian GEN II MBE system and consisted of the following layers: 1.1 μm of undoped GaAs followed by a 200-Å undoped Al_{0.33}Ga_{0.67}As spacer, a 400-Å Al_{0.33}Ga_{0.67}As doped with 10¹⁸ cm⁻³ Si, and finally a 170-Å GaAs cap. The lithographic pattern (the solid parts in the figure) was defined with an electron beam in PMMA and subsequently etched with a H₂SO₄:H₂O₂:H₂O mixture to a depth of about 700 Å thus defining a number of narrow constrictions of about 0.8 μm in width and 1-μm separation. Alloyed Au_xGe_{1-x}Ni Ohmic contacts allowed resistance measurements to be taken.

The design of the pattern allows the electron orbit to be analyzed as a function of angle between the $[01\bar{1}]$ and $[\bar{2}33]$ directions. A magnetic field is applied to direct a ballistic cone of electrons from an emitter to a collector. If the Fermi surface is warped in any way due to a modification in band structure, then the classical cyclo-

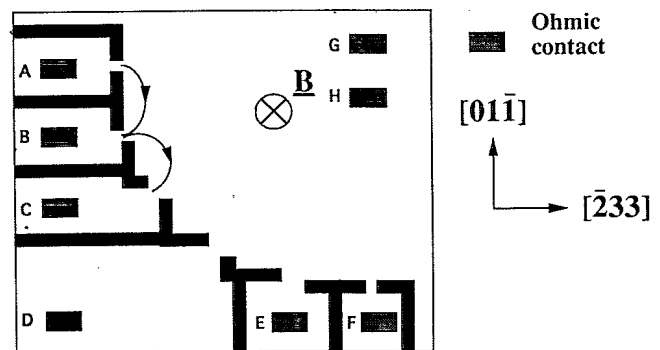


FIG. 1. A schematic representation of the device showing lithographical defined constrictions (the solid regions) and Ohmic contacts A-H for current and voltage probes. Electron orbits are indicated for two different measurement angles.

tron orbit will be modified instead of the normal circular orbit for isotropic systems. The device design allows us to measure the diameter of the cyclotron orbit for a given magnetic field at five different cross sections.

The experiment was carried out at 1.7 K, a temperature at which quantum interference effects can be ignored, and the sample was illuminated prior to measurement. Using lock-in techniques, a current of 100 nA is passed between one of the constrictions acting as the emitter (contacts $A-G$), then a voltage is measured across an adjacent constriction ($B-H$), the collector, and all other voltage probes are grounded to stop stray charging effects. A magnetic field is then applied to obtain the transverse magnetic-focusing spectrum. As the magnetic field is increased a series of oscillations across the voltage probes is observed. The first oscillation corresponds to a magnetic field B , where the electron wave vector $\mathbf{k} = \pi BeL/h$, where L is the vector length between the two constrictions; that is, exactly half a classical cyclotron orbit traverses the two adjacent constrictions (see one of the orbits marked on Fig. 1). The further oscillations at higher field correspond to multiple skipping orbits along the edge of the lithographic region between the constrictions, where $\mathbf{k} = n\pi BeL/h$, for $n = 2, 3, \dots, \infty$. At higher fields, Shubnikov-de Haas oscillations are observed, these were used to determine the carrier density; for these measurements the carrier density was $4.5 \times 10^{11} \text{ cm}^{-2}$. Figure 2 shows a plot of \mathbf{k} as a function of angle for two samples from the same wafer. Independent Hall and resistivity measurements from this wafer give mobilities of 1.04×10^6 and $1.43 \times 10^6 \text{ cm}^2 \text{ V}^{-1} \text{ s}^{-1}$ for $[01\bar{1}]$ and $[\bar{2}33]$ directions, respectively, for the same corresponding carrier density. It can be seen to within experimental error that the electron wave vector $|\mathbf{k}|$ lies on a circle; this can be compared to the result of Heremans, Santos, and Shayegan,⁹ which showed an elliptical contour for hole wave vectors. Heremans, Santos, and Shayegan explained their results by introducing an anisotropic effective mass induced by a periodic modulation in band structure, which they surmised could be due to surface corrugations on the (311) substrate which have been reported elsewhere.¹¹ This can explain the anisotropic wave-vector contour and mobilities, the mobility being derived through the empirical relation $\mu = e\tau/m^*$. In our case, we observe anisotropy in the mobilities but not in the effective electron mass. This confirms our earlier prediction that the anisotropic mobility is caused purely through an empirical scattering time τ and not an effective mass m^* .¹⁰

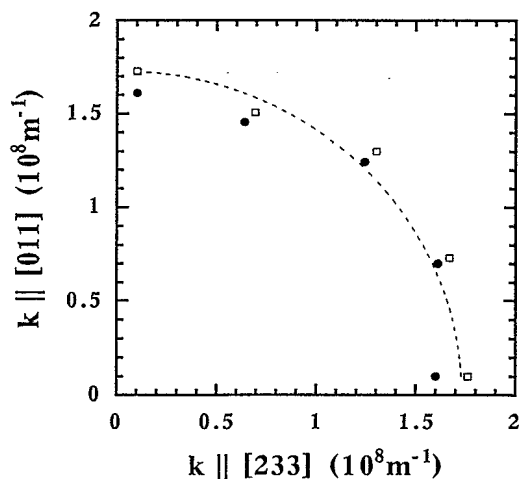


FIG. 2. Values of the electron wave vector are plotted as a function of different measurement angles for two different samples \bullet and \square . A circle is plotted to demonstrate that the Fermi surface is isotropic.

tropic effective mass induced by a periodic modulation in band structure, which they surmised could be due to surface corrugations on the (311) substrate which have been reported elsewhere.¹¹ This can explain the anisotropic wave-vector contour and mobilities, the mobility being derived through the empirical relation $\mu = e\tau/m^*$. In our case, we observe anisotropy in the mobilities but not in the effective electron mass. This confirms our earlier prediction that the anisotropic mobility is caused purely through an empirical scattering time τ and not an effective mass m^* .¹⁰

A further measurement was carried out to determine the ballistic length for the electrons. The contacts to the device were then reconfigured so that a constriction at one end of the device was used as an emitter (contacts $A-G$) and sequentially all other constrictions were used as collectors ($B-H$, $C-H$, etc.). Thus electrons are emitted from A and are collected either in B , C , D , E , and F . Electron-focusing spectra were obtained for different electron orbit lengths. Analyzing the amplitude of the focused electrons as a function of length results in a length scale that is related to the ballistic length of the electrons. Figure 3 shows a plot of electron-focus amplitude as a function of path length. It can be seen that the amplitude of the focused electrons has a functional form of $\exp(-L/\lambda_b)$, where λ_b is determined from the graph to be between 2.2 and 2.5 μm ; this is somewhat dependent on the sample. We noted that as the electron trajectories are parts of circular orbits, the electron will travel the same distance in both $[01\bar{1}]$ and $[\bar{2}33]$ directions, thus the value of λ_b is an average in the two orthogonal direc-

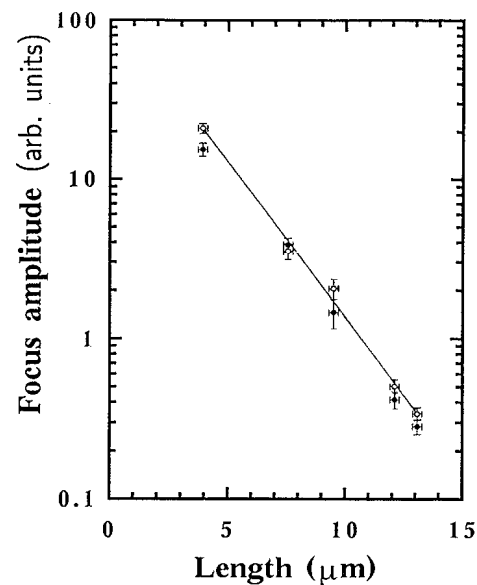


FIG. 3. Focus amplitude for spectra are plotted as a function of path length for two different samples \bullet and \circ . The injector current was from contacts $A-G$, while the voltage probes were $H-B$, C , D , E , and F , respectively. The exponential dependence on distance allows a ballistic length to be determined. λ_b is found to be between 2.2 and 2.5 μm , depending on the sample.

tions. In order to investigate the ballistic length in orthogonal directions it will be necessary to devise another sample design that does not involve the use of magnetic fields. The elastic mean free path λ_f , determined from the mobility and carrier density, has values of 10.9 and 15 μm , respectively, for the two directions. These values are much larger than the measured value of λ_b ; however, this is typical of such measurements⁶ since the length we measure is connected with the ballistic nature of a cone of electrons emanating from a constriction. The mean free path calculated from mobility values gives an average length between large-angle scattering processes, but it is likely that the ballistic length depends on different criteria, for example the inclusion of some small-angle scattering processes. However, a length calculated from a single-particle scattering or Dingle time τ_q , which does include small-angle scattering, is found to be 0.29 μm [using a carrier density of $4.5 \times 10^{11} \text{ cm}^{-2}$ and a value of $\tau_q = 0.99 \text{ psec}$ (Ref. 10)]. Thus we see that the ballistic length lies between the mean free path and the path of one calculated from Shubnikov-de Haas oscillations.

In summary, we have shown that electron focusing can be carried out on 2DEG's formed on (311)B-orientated

wafers. The 2DEG's show anisotropic transport properties, having higher mobilities in the [233] direction than the [011] direction. However, in determining the mobility, the focusing experiment indicates that the effective mass is isotropic, and thus we infer, an anisotropic carrier scattering time τ . This result would point against a band-structure modulation by surface corrugations as reported by Heremans, Santos, and Shayegan,⁹ but support anisotropic carrier scattering from, for example, interface roughness scattering.¹⁰ Although the two systems may be different, as Heremans, Santos, and Shayegan have studied the A (or Ga-rich) surface and we have studied the As-rich surface, at the moment there seems to be little evidence that the two surfaces are special cases.¹¹ The ballistic length for electrons in the 2DEG was also determined at 1.7 K and found to be between 2.2 and 2.5 μm , as reported previously in similar experiments. This length is a factor of 3–4 smaller than the calculated mean free path λ_f .

We would like to acknowledge the support of the SERC, and D.A.R., acknowledges financial support from Toshiba Cambridge Research Centre Limited.

¹V. S. Tsoi, Pis'ma Zh. Eksp. Teor. Fiz. **19**, 114 (1974) [JETP Lett. **19**, 70 (1974)].

²V. S. Tsoi and X. Razgonov, Zh. Eksp. Teor. Fiz. **74**, 1137 (1978) [Sov. Phys. JETP **47**, 597 (1978)].

³F. Nihey, K. Nakamura, M. Kuzuhara, N. Samato, and T. Itoh, Appl. Phys. Lett. **57**, 1218 (1990).

⁴L. W. Molenkamp, M. J. P. Brugmans, K. W. van Houten, and C. T. Foxon, Semicond. Sci. Technol. **7**, 228 (1992).

⁵Y. Oowaki, J. E. F. Frost, L. Martin-Moreno, M. Pepper, D. A. Ritchie, and G. A. C. Jones, Phys. Rev. B **47**, 4088 (1993).

⁶J. Spector, J. S. Weiner, H. L. Störmer, K. W. Baldwin, L. N. Pfeiffer, and K. W. West, Surf. Sci. **228**, 283 (1989).

⁷J. Spector, J. S. Weiner, H. L. Störmer, K. W. Baldwin, L. N. Pfeiffer, and K. W. West, Surf. Sci. **263**, 240 (1992).

⁸K. Tsukagoshi, S. Takaoka, K. Murage, K. Gamo, and S. Namba, Appl. Phys. Lett. **62**, 1609 (1993).

⁹J. J. Heremans, M. B. Santos, and M. Shayegan, Surf. Sci. **305**, 348 (1994).

¹⁰A. C. Churchill, G. H. Kim, A. Kurobe, M. Y. Simmons, D. A. Ritchie, M. Pepper, and G. A. C. Jones, J. Phys. Condens. Matter **6**, 6131 (1994).

¹¹R. Nötzel, L. Däweritz, and K. Ploog, J. Cryst. Growth **127**, 858 (1993); L. Däweritz, J. Cryst. Growth **127**, 949 (1993).